



**FIRST INTERNATIONAL SCHOOL
OF HADRON FEMTOGRAPHY**

Jefferson Lab | September 16 - 25, 2024

Experimental Methods

Sep 21st 2024

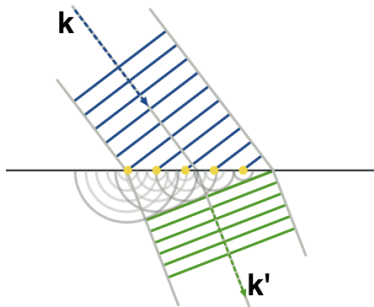
F.-X. Girod

Lecture 3
with Charles Hyde



Diffraction and Imaging

Huygens-Kirchhoff-Fresnel principle



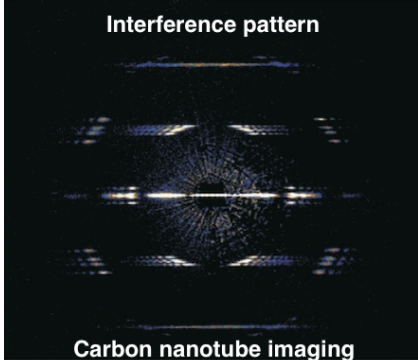
$$\vec{q} = \vec{k} - \vec{k}'$$

The interference pattern is given by the superposition of spherical wavelets

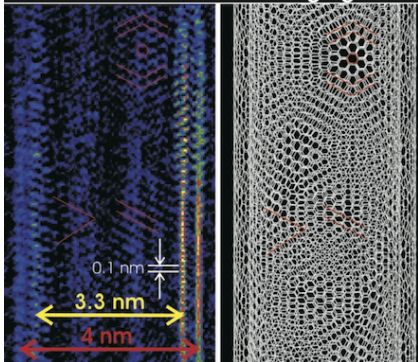
$$f(\Omega_{\vec{q}}) = \int \frac{d^3\vec{r}}{(2\pi)^3} F(\vec{r}) e^{i\vec{q}\cdot\vec{r}}$$

Fourier imaging

Interference pattern



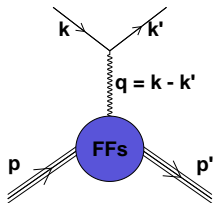
Carbon nanotube imaging



Elastic scattering

Form Factors

Probing deeper using virtual photons



$$J_{EM}^{\mu} = F_1 \gamma^{\mu} + \frac{\kappa}{2M} F_2 i \sigma^{\mu\nu} q_{\nu}$$

$$\frac{d\sigma}{d\Omega} = \frac{\sigma_{\text{Mott}}}{\epsilon(1+\tau)} [\tau G_M^2 + \epsilon G_E^2]$$

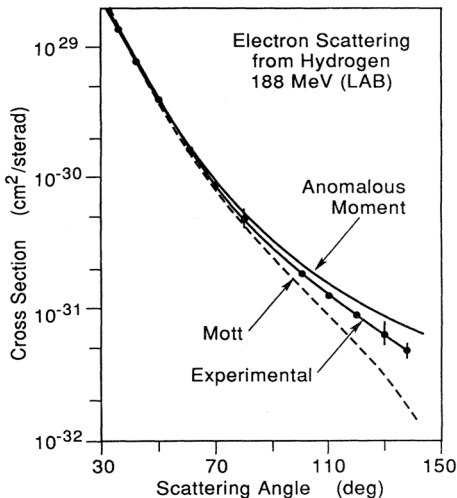
$$\tau = \frac{Q^2}{4M^2}$$

$$Q^2 = -(k - k')^2 = -m_{\gamma^*}^2$$

$$\frac{1}{\epsilon} = 1 + 2(1 + \tau) \tan^2 \frac{\theta_e}{2}$$

$$G_E = F_1 - \tau F_2$$

$$G_M = F_1 + F_2$$



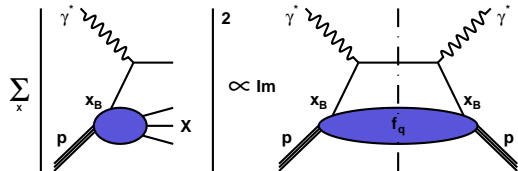
Hofstadter Nobel prize 1961

"The best fit in this figure indicates
an rms radius close to $0.74 \pm 0.24 \times 10^{-13}$ cm."

Imaging in transverse impact parameter space

Deeply Inelastic Scattering

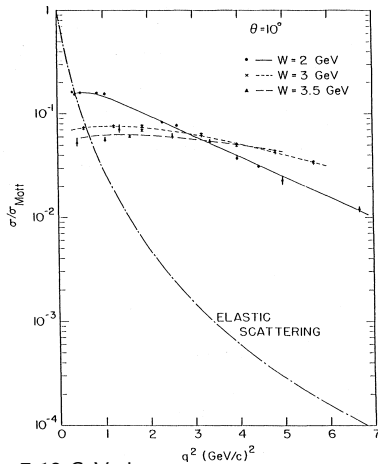
Parton Distributions



The total cross section is given by the imaginary part of the forward amplitude

$$\nu = E_{\gamma^*} \quad , \quad x_B = \frac{Q^2}{2M\nu}$$

$\sigma_{\text{DIS}}(x_B, Q^2) \rightarrow$ scaling, point-like constituents



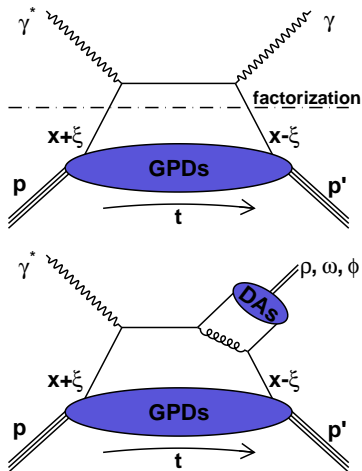
Discovery of quarks, SLAC-MIT group, 7-18 GeV electron
Friedman, Kendall, Taylor, Nobel prize 1990

$$\lim_{Q^2 \rightarrow \infty} \sigma_{\text{DIS}}(x_B) = \int_{x_B}^1 \frac{d\xi}{\xi} \sum_a f_a(\xi, \mu) \hat{\sigma}^a \left(\frac{x_B}{\xi}, \frac{Q}{\mu} \right)$$

1-D distribution in longitudinal momentum space

Deep Exclusive Scattering

Generalized Parton Distributions



$$\gamma^* p \rightarrow \gamma p', \quad \gamma^* p \rightarrow \begin{cases} \rho p' \\ \omega p' \\ \phi p' \end{cases}$$

Bjorken regime :
 $Q^2 \rightarrow \infty, x_B$ fixed

$$t \text{ fixed} \ll Q^2, \quad \xi \rightarrow \frac{x_B}{2-x_B}$$

$$\frac{P^+}{2\pi} \int dy^- e^{ixP^+y^-} \langle p' | \bar{\psi}_q(0) \gamma^+ (1 + \gamma^5) \psi(y) | p \rangle$$

$$= \bar{N}(p') \left[H^q(x, \xi, t) \gamma^+ + E^q(x, \xi, t) i\sigma^{+\nu} \frac{\Delta_\nu}{2M} \right. \\ \left. + \tilde{H}^q(x, \xi, t) \gamma^+ \gamma^5 + \tilde{E}^q(x, \xi, t) \gamma^5 \frac{\Delta^+}{2M} \right] N(p)$$

spin	N no flip	N flip
q no flip	H	E
q flip	\tilde{H}	\tilde{E}

3-D Imaging conjointly in transverse impact parameter **and** longitudinal momentum

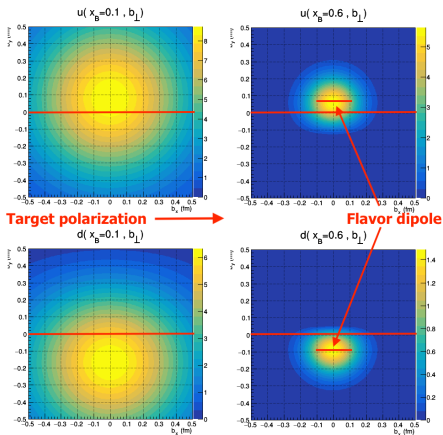
GPDs and Transverse Imaging

(x_B, t) correlations

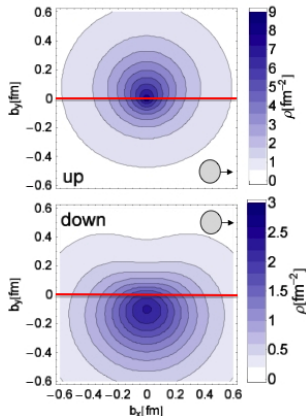
$$q_X(x, \vec{b}_\perp) = \int \frac{d^2 \vec{\Delta}_\perp}{(2\pi)^2} \left[H(x, 0, t) - \frac{E(x, 0, t)}{2M} \frac{\partial}{\partial b_y} \right] e^{-i \vec{\Delta}_\perp \cdot \vec{b}_\perp}$$

M. Burkardt, Int. J. Mod. Phys. **A 18** 173 (2003)

QCDSF coll. PRL**98** 222001 (2007)



Lattice calculation



Energy Momentum Tensor

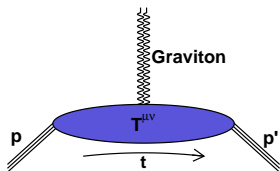
Gravitational Form Factors definition :

$$\langle p' | \hat{T}_{\mu\nu}^q | p \rangle = \bar{N}(p') \left[M_2^q(t) \frac{P_\mu P_\nu}{M} + J^q(t) \frac{i(P_\mu \sigma_{\nu\rho} + P_\nu \sigma_{\mu\rho}) \Delta^\rho}{2M} + d_1^q(t) \frac{\Delta_\mu \Delta_\nu - g_{\mu\nu} \Delta^2}{5M} \right] N(p)$$

Confinement forces from space-space components of EMT

The graviton with spin 2 couples directly to EMT

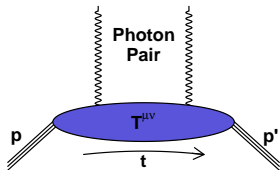
But gravity is too weak to produce count rates in the detector



We can construct a spin 2 operator using two spin 1 operators

→ use a process with two photons to measure the EMT?

X. Ji *PRL***78** 610 (1997) ; M. Polyakov *PLB***555** 57 (2003)



GPDs and Energy Momentum Tensor

(x, ξ) correlations

Form Factors accessed *via* second x-moments :

$$\langle p' | \hat{T}_{\mu\nu}^q | p \rangle = \bar{N}(p') \left[M_2^q(t) \frac{P_\mu P_\nu}{M} + J^q(t) \frac{i(P_\mu \sigma_{\nu\rho} + P_\nu \sigma_{\mu\rho}) \Delta^\rho}{2M} + d_1^q(t) \frac{\Delta_\mu \Delta_\nu - g_{\mu\nu} \Delta^2}{5M} \right] N(p)$$

Angular momentum distribution

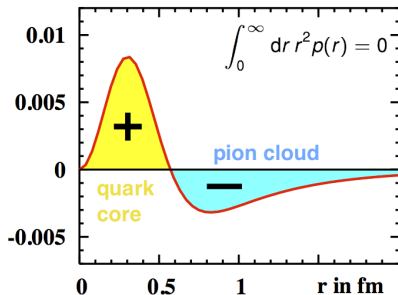
$$J^q(t) = \frac{1}{2} \int_{-1}^1 dx x [H^q(x, \xi, t) + E^q(x, \xi, t)]$$

Mass and force/pressure distributions

$$M_2^q(t) + \frac{4}{5} d_1^q(t) \xi^2 = \frac{1}{2} \int_{-1}^1 dx x H^q(x, \xi, t)$$

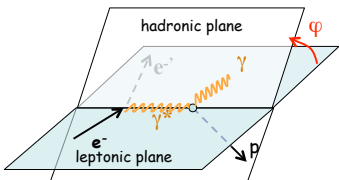
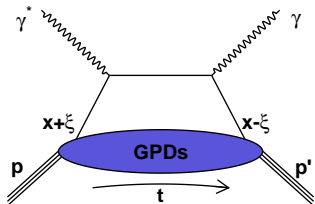
$$d_1(t) = 15M \int d^3\vec{r} \frac{j_0(r\sqrt{-t})}{2t} p(r)$$

Distribution of pressure
 $r^2 p(r)$ in GeV fm^{-1}



Deeply Virtual Compton Scattering

The cleanest GPD probe at low and medium energies



$$ep \rightarrow ep\gamma$$

$$\sigma(ep \rightarrow ep\gamma) \propto \left| \begin{array}{c} \text{DVCS} \\ \text{(a)} \end{array} + \begin{array}{c} \text{BH} \\ \text{(b)} + \text{(c)} \end{array} \right|^2$$

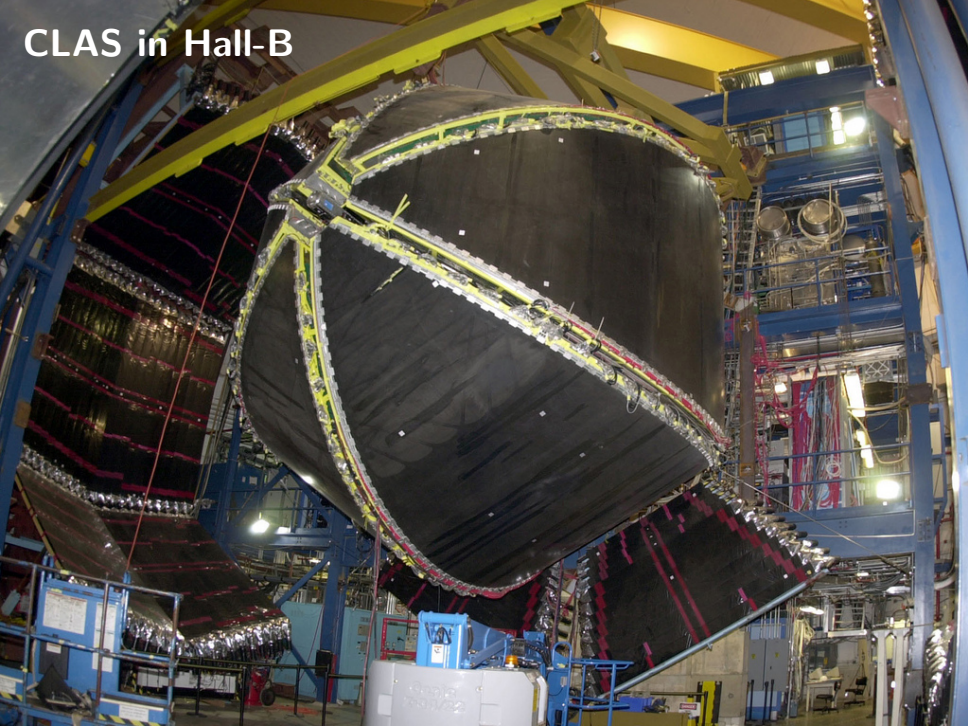
$$A_{LU} = \frac{d^4\sigma^{\rightarrow} - d^4\sigma^{\leftarrow}}{d^4\sigma^{\rightarrow} + d^4\sigma^{\leftarrow}} \stackrel{\text{twist-2}}{\approx} \frac{\alpha \sin \phi}{1 + \beta \cos \phi}$$

$$\alpha \propto \text{Im} \left(F_1 \mathcal{H} + \xi G_M \tilde{\mathcal{H}} - \frac{t}{4M^2} F_2 \mathcal{E} \right)$$

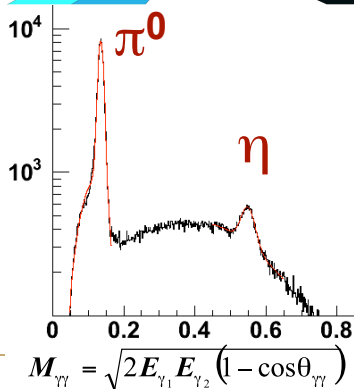
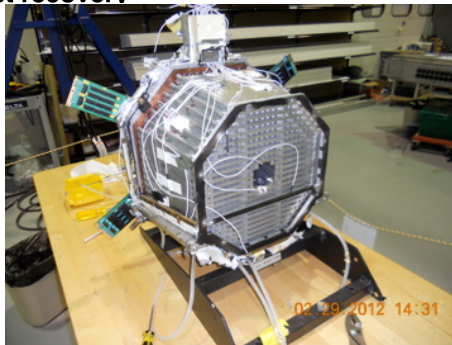
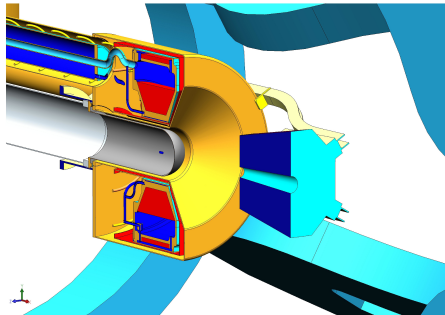
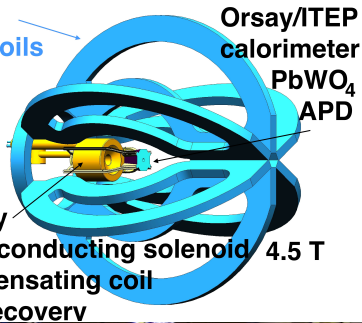
$$\mathcal{H}(\xi, t) = i\pi H(\xi, \xi, t) + \mathcal{P} \int_{-1}^1 dx \frac{H(x, \xi, t)}{x - \xi}$$

$$A_{UL} \propto \text{Im} \left(F_1 \tilde{\mathcal{H}} + \xi G_M \mathcal{H} + G_M \frac{\xi}{1 + \xi} \mathcal{E} + \dots \right) \sin \phi$$

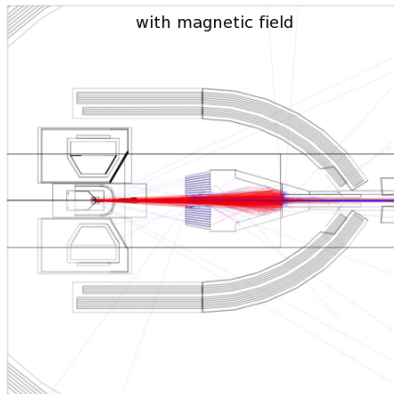
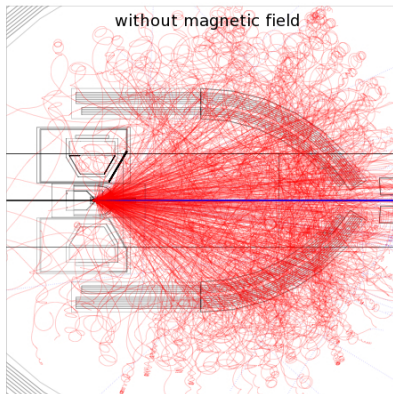
CLAS in Hall-B



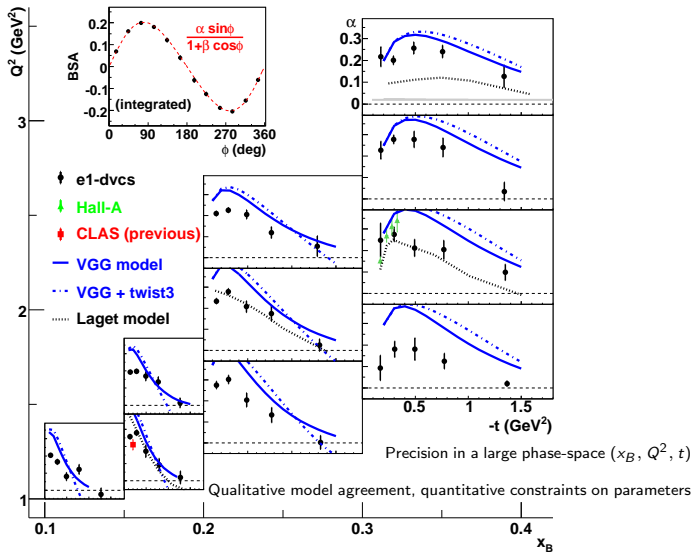
CLAS
torus coils



Solenoid and Inner Calorimeter

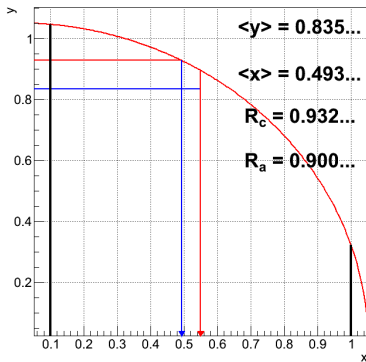
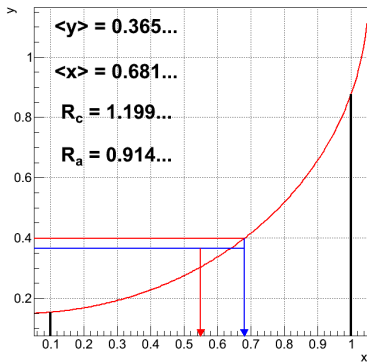


CLAS proton Beam Spin Asymmetry



F.-X. G. *et al.*, PRL **100** (2008) 162002

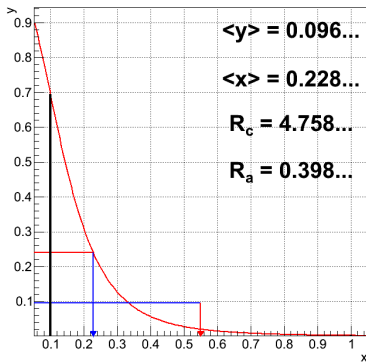
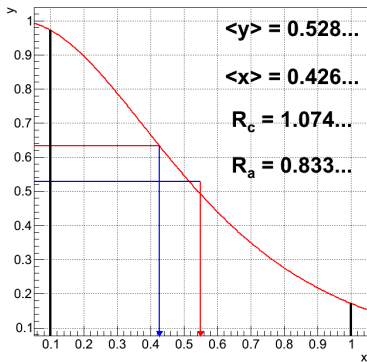
Finite Bin Size Corrections



Bin volume
 Average value (observable) in bin
 Bin center
 Bin average

$$\begin{aligned}
 V &= \int_{\text{bin}} dx \\
 \langle y \rangle &= y_a = \frac{1}{V} \int_{\text{bin}} y(x) dx \\
 x_c &= \frac{1}{V} \int_{\text{bin}} x dx \\
 \langle x \rangle &= x_a = \frac{1}{Vy_a} \int_{\text{bin}} xy(x) dx
 \end{aligned}$$

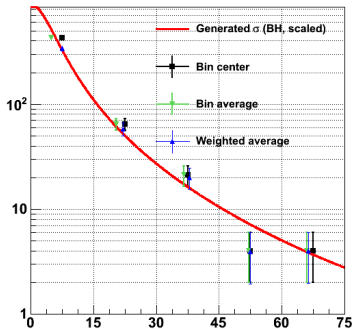
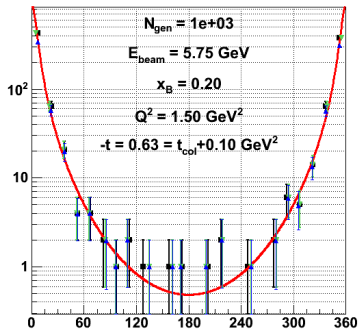
Finite Bin Size Corrections



Bin volume
 Average value (observable) in bin
 Bin center
 Bin average

$$\begin{aligned}
 V &= \int_{\text{bin}} dx \\
 \langle y \rangle &= y_a = \frac{1}{V} \int_{\text{bin}} y(x) dx \\
 x_c &= \frac{1}{V} \int_{\text{bin}} x dx \\
 \langle x \rangle &= x_a = \frac{1}{Vy_a} \int_{\text{bin}} xy(x) dx
 \end{aligned}$$

Finite Bin Size Corrections



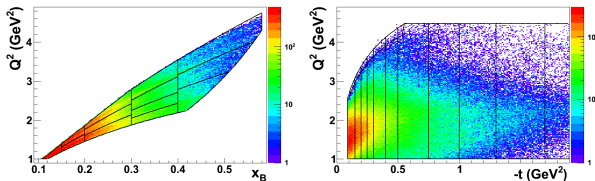
Bin volume
 Average value (observable) in bin
 Bin center
 Bin average

$$\begin{aligned}
 V &= \int_{\text{bin}} dx \\
 \langle y \rangle &= y_a = \frac{1}{V} \int_{\text{bin}} y(x) dx \\
 x_c &= \frac{1}{V} \int_{\text{bin}} x dx \\
 \langle x \rangle &= x_a = \frac{1}{V y_a} \int_{\text{bin}} x y(x) dx
 \end{aligned}$$

CLAS proton cross-section



More than 3k bins

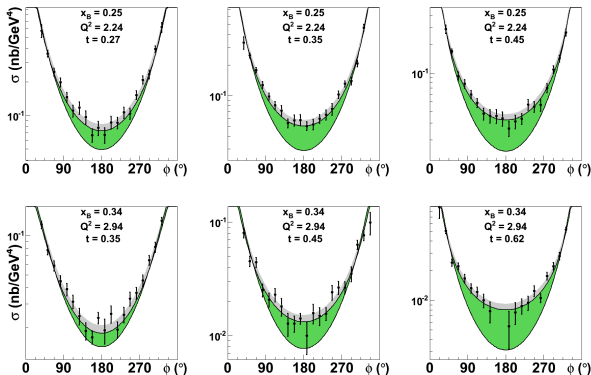


Dispersion relation :

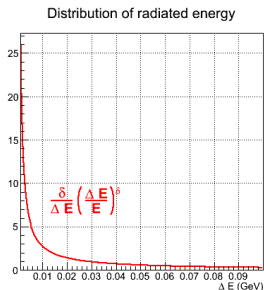
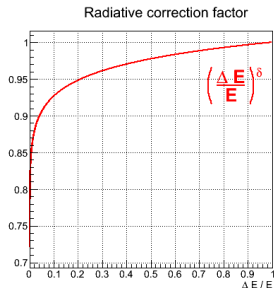
$$\text{Re } \mathcal{H} = \left[\int \text{Im } \mathcal{H} \right] + \Delta$$

green band shows
difference with BH

→ sensitivity to d_1



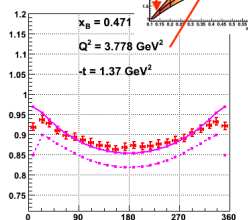
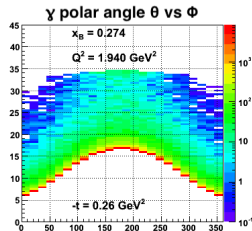
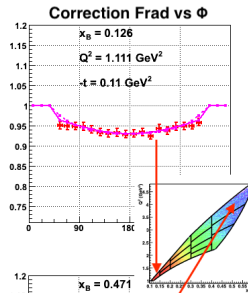
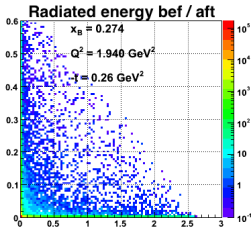
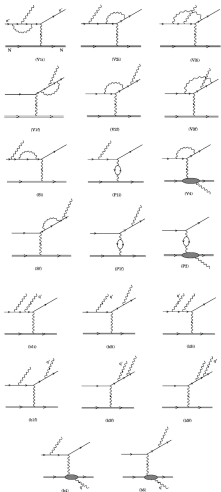
Radiative corrections (semiclassical)



$$\left. \frac{d\sigma}{d\Omega} \right|_{\text{meas}} = (1 + \delta_{\text{virt}} + \delta_{\text{real}}) \left. \frac{d\sigma}{d\Omega} \right|_{\text{Born}}, \quad \delta_{\text{real}} = \ln \left(\frac{\Delta E}{E} \right)^\delta, \quad \delta = \frac{2\alpha}{\pi} \left[\ln \frac{Q^2}{m^2} - 1 \right]$$

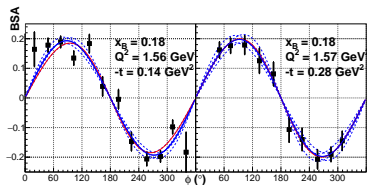
Schwinger resummation : $1 + \delta_{\text{real}} \rightarrow e^{\delta_{\text{real}}}$, $\left. \frac{d\sigma}{d\Omega} \right|_{\text{meas}} = \left. \frac{d\sigma}{d\Omega} \right|_{\text{Born}} (1 + \delta_{\text{virt}}) \left(\frac{\Delta E}{E}\right)^\delta$

DVCS Radiative Corrections Fast MC



M. Vanderhaeghen *et al.*, Phys. Rev **C62** (2000) 025510
 I. Akushevich & A. Ilyichev Phys. Rev **D98** (2018) 013005

Global Fits to extract the D-term



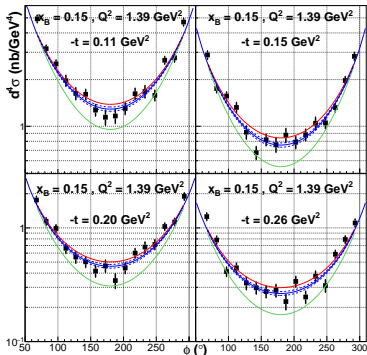
Beam Spin Asymmetries

$$\text{Im}\mathcal{H}(\xi, t) = \frac{N}{1+x} \left(\frac{2\xi}{1+\xi} \right)^{-\alpha_R(t)} \left(\frac{1-\xi}{1+\xi} \right)^b \left(\frac{1-\xi}{1+\xi} \frac{t}{M^2} \right)^{-1}$$

Unpolarized cross-sections

Use dispersion relation:

$$\text{Re}\mathcal{H}(\xi, t) = \Delta + \mathcal{P} \int dx \left(\frac{1}{\xi - x} - \frac{1}{\xi + x} \right) \text{Im}\mathcal{H}(\xi, t)$$

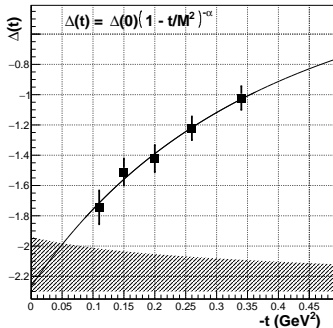


pure Bethe-Heitler

local fit + uncertainty range

resulting global fit

DVCS Dispersion: subtraction constant results



$$\text{Im}\mathcal{H}(\xi, t) = \frac{N}{1+x} \left(\frac{2\xi}{1+\xi} \right)^{-\alpha_R(t)} \left(\frac{1-\xi}{1+\xi} \right)^b \left(\frac{1-\xi}{1+\xi} \frac{t}{M^2} \right)^{-1}$$

α_R is fixed from small- x Regge phenomenology

b is a free parameter for the large x behavior

p is fixed to 1 for the valence

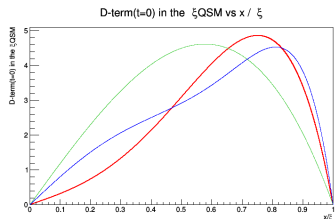
M is a free parameter controlling the t dependence

$$\Delta(t) = \Delta(0) \left(1 - \frac{t}{M^2} \right)^{-\alpha} = 2 \int_{-1}^1 dz \frac{D(z, t)}{1-z}$$

$$D(z, t) = (1-z^2) \sum_{k=1}^{\infty} \left[e_u^2 d_{2k-1}^u(t) + e_d^2 d_{2k-1}^d(t) \right] C_{2k-1}^{3/2}(z)$$

Hereafter assume $d_{2k-1}^u \approx d_{2k-1}^d$

Separation of the GFF d_1



In the χ QSM:

$$d_1(0) \approx -4.0; d_3(0) \approx -1.2; d_5(0) \approx -0.4$$

$$H(x, \xi, t) = \dots + \theta \left[1 - \frac{x^2}{\xi^2} \right] D\left(\frac{x}{\xi}, t\right)$$

$$D(z, t) = (1 - z^2) \left[d_1(t) C_1^{3/2}(z) + d_3(t) C_3^{3/2}(z) + \dots \right]$$

$$C_1^{3/2}(z) = 3z$$

$$C_3^{3/2}(z) = \frac{5}{2} (7z^3 - 3z)$$

$$C_5^{3/2}(z) = \frac{21}{8} (33z^5 - 30z^3 + 5z)$$

To separate orthogonal Gegenbauer polynomials:

requires measurement of (x, ξ) dependence (or at least $z = x/\xi$ dependence)
different reaction such as DDVCS, will require higher luminosity

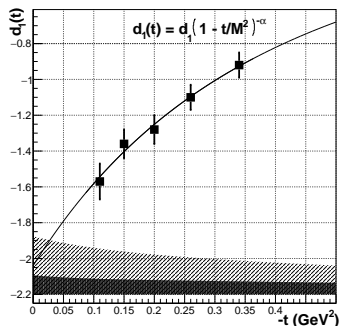
For now, to make progress it is necessary to make assumptions

Use guidance from models such as χ QSM or lattice results

Also implement constraints from theory into phenomenological fits

Separation of the GFF d_1

$$D^q\left(\frac{x}{\xi}, t\right) = \left(1 - \frac{x^2}{\xi^2}\right) \left[d_1^q(t) C_1^{3/2}\left(\frac{x}{\xi}\right) + d_3^q(t) C_3^{3/2}\left(\frac{x}{\xi}\right) + \dots \right]$$



t -dependence of the D-term :

Dipole gives singular pressure at $r = 0$

Power law implied by counting rules?

Exponential?

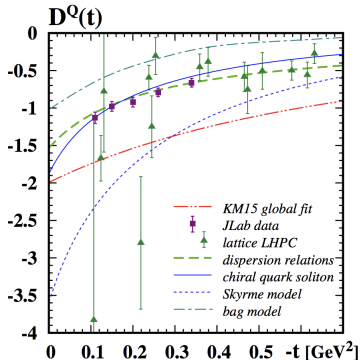
...

$d_1(0) < 0$ dynamical **stability** of bound state

$$d_1(0) = -2.04 \pm 0.14 \pm 0.33$$

First Measurement of new fundamental quantity

D-term comparison with theory



Dispersion Relation Analysis
 Chiral quark soliton model
 Lattice results LHPC
 Global fit

M. V. Polyakov, P. Schweitzer Int.J.Mod.Phys. **A33** (2018)

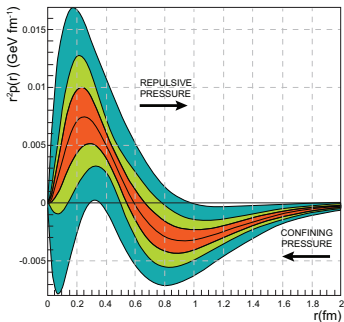
em: $\partial_\mu J_{\text{em}}^\mu = 0$	$\langle N' J_{\text{em}}^\mu N \rangle$	\longrightarrow	$Q = 1.602176487(40) \times 10^{-19} \text{C}$ $\mu = 2.792847356(23) \mu_N$
---	--	-------------------	---

weak: PCAC	$\langle N' J_{\text{weak}}^\mu N \rangle$	\longrightarrow	$g_A = 1.2694(28)$ $g_p = 8.06(55)$
-------------------	--	-------------------	--

gravity: $\partial_\mu T_{\text{grav}}^{\mu\nu} = 0$	$\langle N' T_{\text{grav}}^{\mu\nu} N \rangle$	\longrightarrow	$m = 938.272013(23) \text{ MeV}/c^2$ $J = \frac{1}{2}$ $D = ?$
---	---	-------------------	--

Proton Pressure distribution results

The pressure at the core of the proton is $\sim 10^{35}$ Pa
About 10 times the pressure at the core of a neutron star



Positive pressure in the core (repulsive force)
Negative pressure at the periphery: pion cloud
Pressure node around $r \approx 0.6$ fm

$$\text{Stability condition : } \int_0^{\infty} dt r^2 p(r) = 0$$

Rooted into Chiral Symmetry Breaking

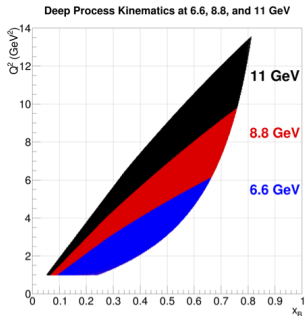
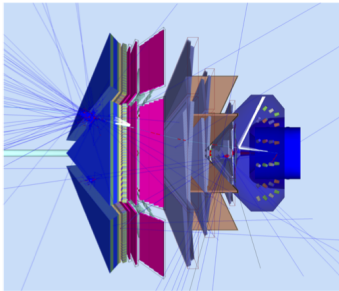
World data fit

CLAS 6 GeV data

Projected CLAS12 data E12-16-010B

DVCS with CLAS12 E12-16-010B

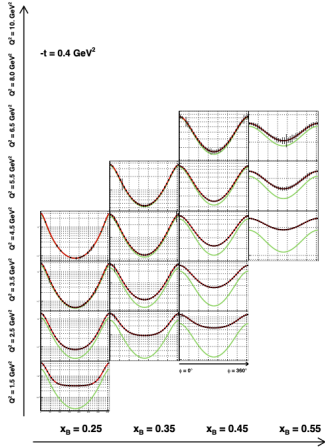
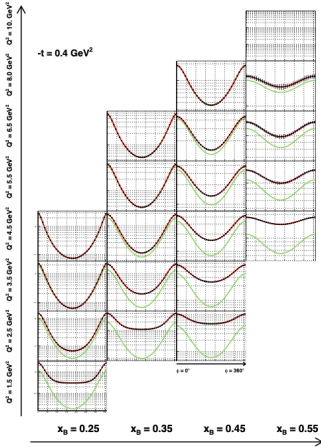
Experimental Configuration



- ▶ $\mathcal{L} = 1 \times 10^{35} \text{ cm}^{-2}\text{s}^{-1}$
- ▶ Inclusive electron trigger (all calibration reactions will be analyzed in parallel)
- ▶ Electrons in the forward detector
- ▶ Protons in the central detector and forward detector
- ▶ Photons in the forward detector and forward tagger

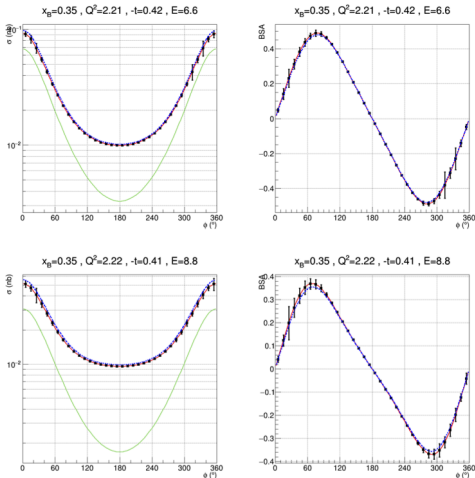
DVCS with CLAS12 E12-16-010B

DVCS Projected Cross Section at 11GeV & 8.8GeV



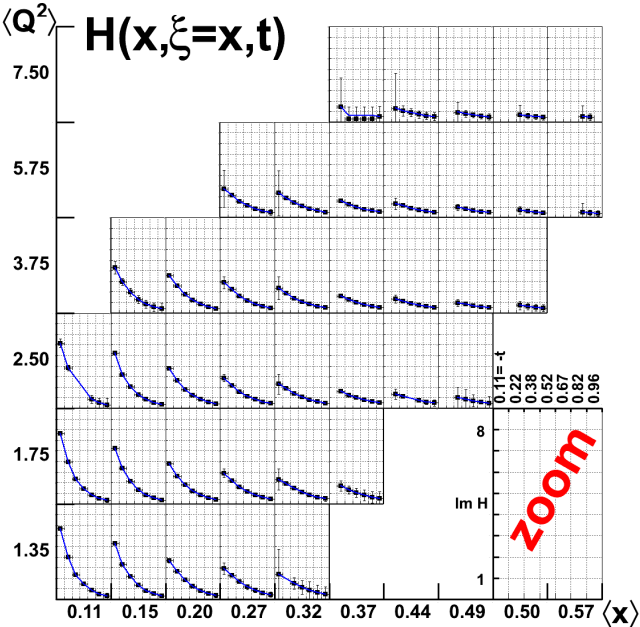
DVCS with CLAS12 E12-16-010B

DVCS Projected Results

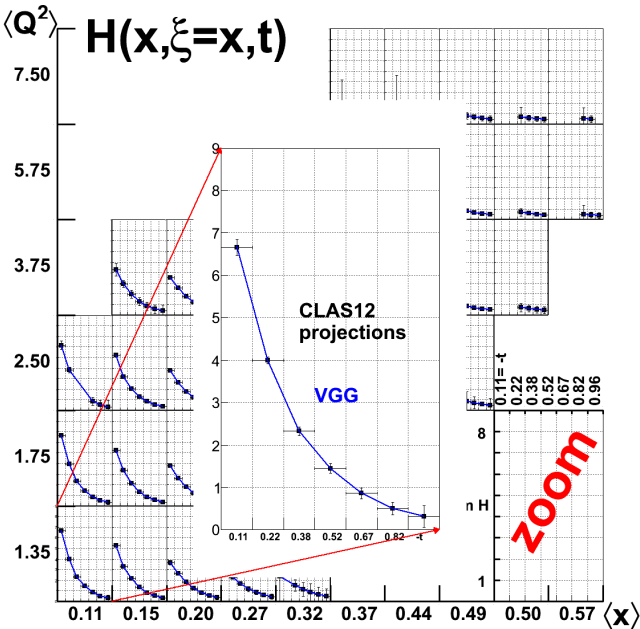


- ▶ Left : cross-sections at fixed kinematics for beam energies 6.6 GeV and 8.8 GeV
- ▶ Right : corresponding Beam Spin Asymmetries
- ▶ Green : pure Bethe-Heitler
- ▶ Red : model fit on 6 GeV data
- ▶ Blue : simultaneous fit of the projected data
- ▶ Separation of :
 $\mathcal{I} \sim 1/y^3$ and $|\mathcal{T}^{\text{DVCS}}|^2 \sim 1/y^2$

Projected impact on GPD extraction methods

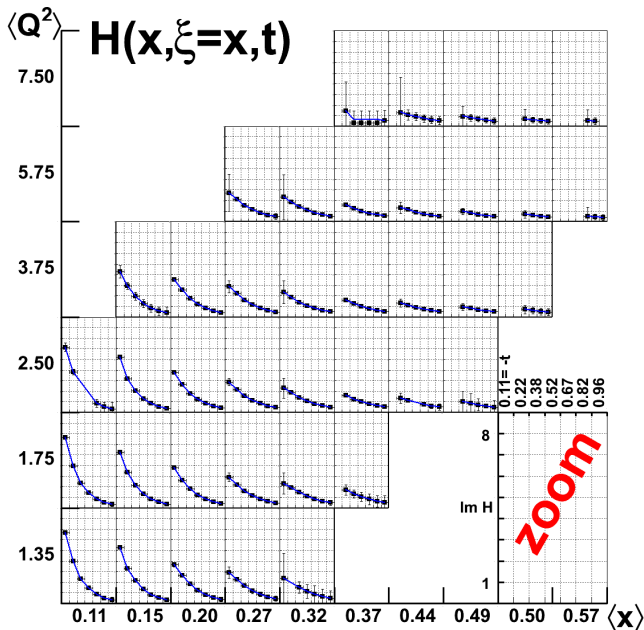


Projected impact on GPD extraction methods

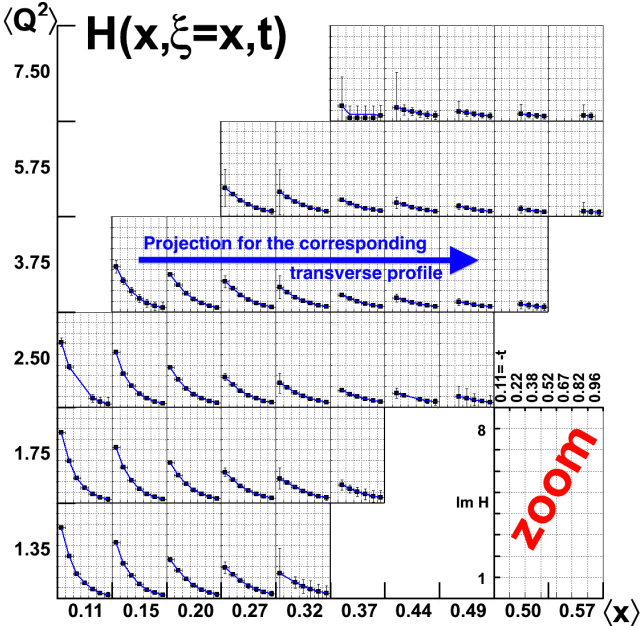


Using simulated data based on VGG model. Input GPD H extracted with good accuracy

Projected impact on GPD extraction methods



Projected impact on GPD extraction methods



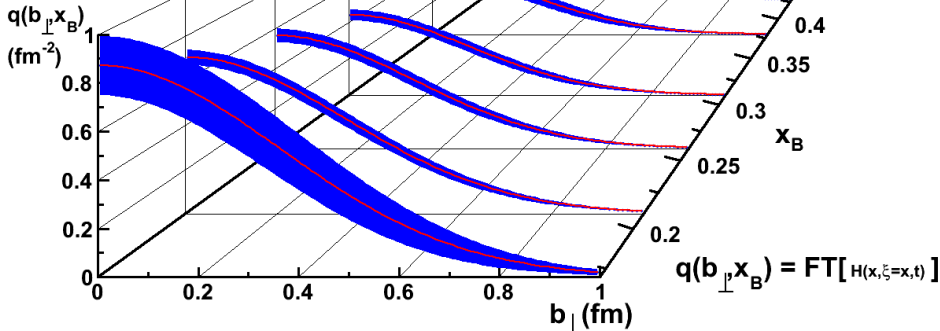
Using simulated data based on VGG model. Input GPD H extracted with good accuracy

Projection for the Nucleon transverse profile

Model profile

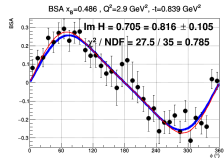
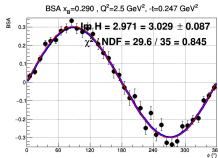
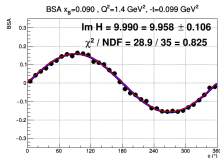
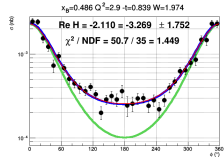
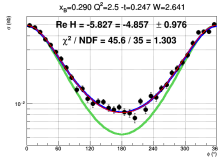
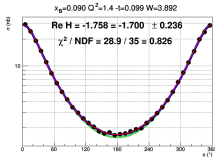
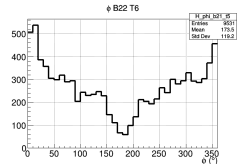
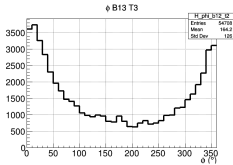
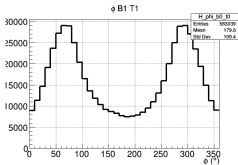
Projected error band

$$Q^2 = 3.75 \text{ GeV}^2$$

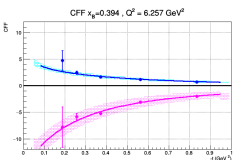
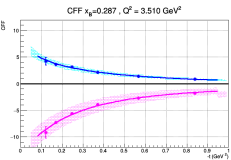
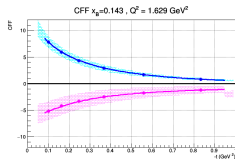
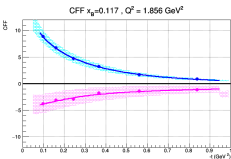


Precision tomography in the valence region

Femtography simulations E12-16-010

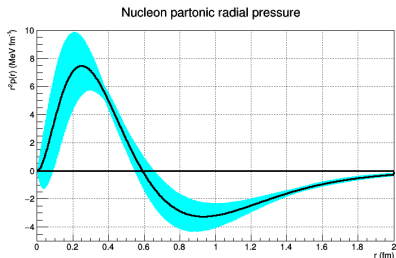
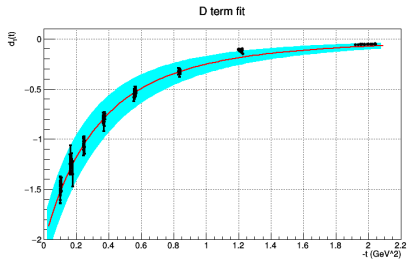


Femtography simulations E12-16-010



High statistics CLAS12 simulations:
sample of extracted Im and Re parts of CFF vs $-t$

Extraction of the D-term, and partonic pressure
from amplitude dispersion global analysis

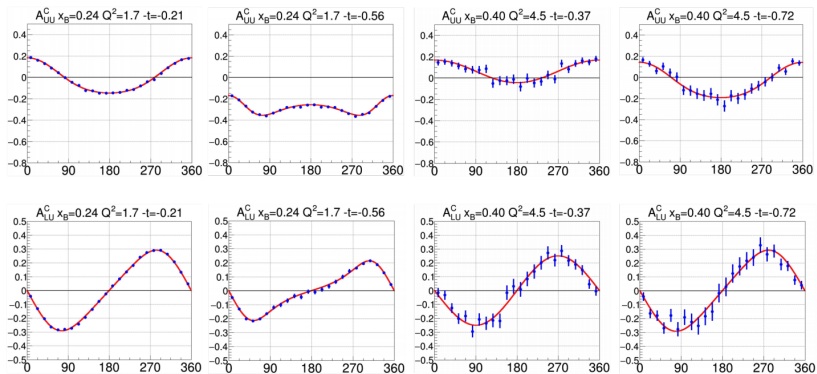


DVCS with a Polarized Positron beam

PEPPo production injecting 60 MeV **100 nA positron polarized at 60%**

(PEPPo Collaboration) D. Abbott *et al.*, PRL116 (2016) 214801 ; L. Cardman *et al.* AIP CP 1970 (2018) 050001

Proposal 100 days (80+20) at $\mathcal{L} = 0.6 \times 10^{35} \text{ cm}^{-2}\text{s}^{-1}$



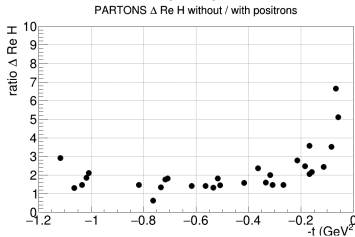
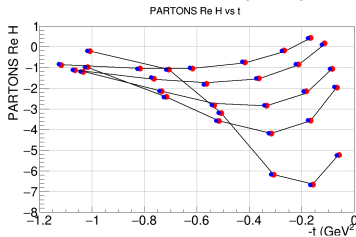
Impact of the CLAS12 Positron data

Global analysis of CLAS12 program observables $\{\sigma_{UU}, A_{LU}, A_{UL}, A_{LL}, A_{UU}^C, A_{LU}^C\}$

unpolarized beam charge asymmetry A_{UU}^C sensitive to the amplitude **real part**

polarized beam charge asymmetry A_{UU}^C sensitive to the amplitude **imaginary part**

Fitting $\{\mathcal{H}, \tilde{\mathcal{H}}\}$ assuming model values for $\{\mathcal{E}, \tilde{\mathcal{E}}\}$

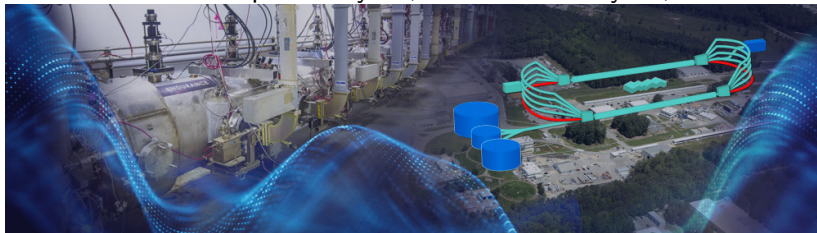


Improvement of the **statistical** and **systematical** uncertainties

Model independent separation of the Interference with BH and DVCS²

Science at the Luminosity Frontier: JLab at 22 GeV

First workshop January 23, 2023 to January 25, 2023

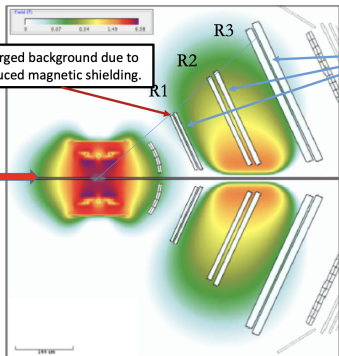


Second workshop



CLAS12 at higher luminosities and energies

- CLAS12 luminosity limited by accidental occupancy of DC R1.



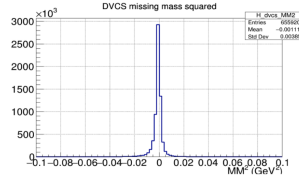
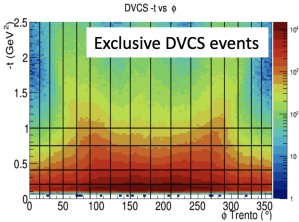
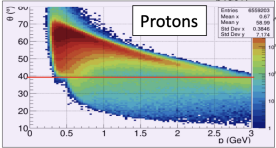
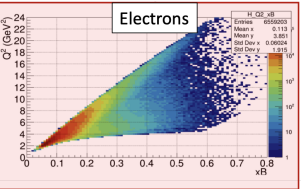
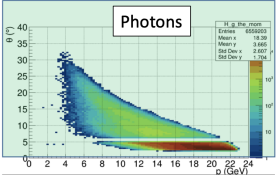
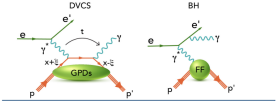
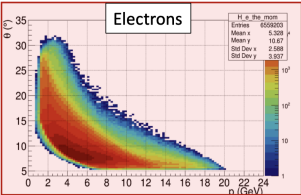
High occupancy in part of R1 limits acceptable operating luminosity.

	R1	R2	R3
CLAS12 @ 11 GeV	2.6%	0.76%	1.18%
CLAS12 @ 24 GeV	2.8%	0.77%	1.23%

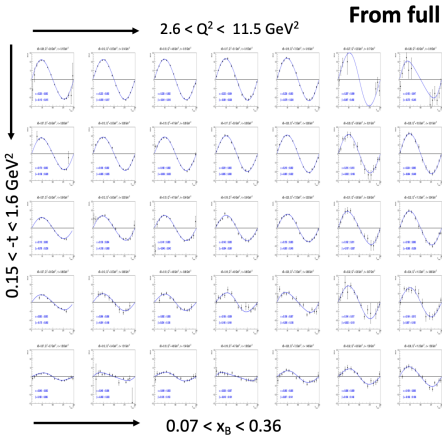
Accidental occupancies increase by less than 10% at 24 GeV compared to 10.6 GeV.

→ higher resolution tracking layers to double luminosity.

DVCS with CLAS at 24 GeV

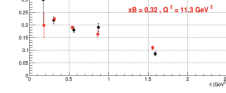
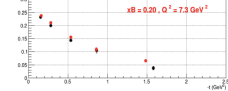
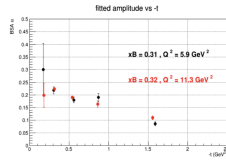
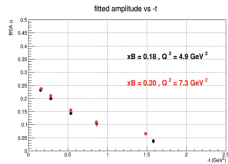
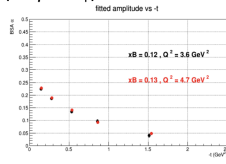
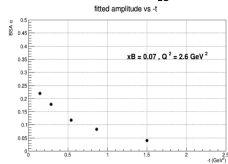


DVCS BSA with CLAS at 24 GeV



From full simulations & reconstructions

$$A_{LU} = \alpha \sin\phi / (1 + \beta \cos 2\phi)$$



Summary - Outlook

- ▶ Dispersive analysis of the DVCS amplitude
- ▶ Access to the Gravitational Form Factors
- ▶ Global analysis with as few parameters as possible
- ▶ Questions about model dependence and systematic uncertainties
- ▶ Rosenbluth separation with several beam energies
- ▶ Direct access to the real part of the amplitude with a positron beam
- ▶ Future prospects: precision at the luminosity and energy frontiers

Next lecture: interplay between JLab and the future Electron Ion Collider

